

Lawrence Berkeley National Laboratory

LBL Publications

Title

Millennial-Scale Vulnerability of the Antarctic Ice Sheet to Regional Ice Shelf Collapse

Permalink

<https://escholarship.org/uc/item/5rs4h36b>

Journal

Geophysical Research Letters, 46(3)

ISSN

0094-8276

Authors

Martin, Daniel F
Cornford, Stephen L
Payne, Antony J

Publication Date

2019-02-16

DOI

10.1029/2018gl081229

Peer reviewed

Geophysical Research Letters

RESEARCH LETTER

10.1029/2018GL081229

Key Points:

- Sustained ice-shelf loss in any of the Amundsen Sea, Ronne, or Ross sectors can lead to wholesale West Antarctic ungrounding and collapse
- Even with extreme forcing, loss is relatively modest for the initial century, increasing markedly after in West Antarctic collapse scenarios
- Modeling suggests Antarctic drainage basins can be assumed to be dynamically independent for one to two centuries before they begin to interact

Supporting Information:

- Supporting Information S1

Correspondence to:

D.F. Martin,
DFMartin@lbl.gov

Citation:

Martin, D. F., Cornford, S. L., & Payne, A. J. (2019). Millennial-scale vulnerability of the Antarctic Ice Sheet to regional ice shelf collapse. *Geophysical Research Letters*, 46, 1467–1475. <https://doi.org/10.1029/2018GL081229>

Received 9 NOV 2018

Accepted 3 JAN 2019

Accepted article online 9 JAN 2019

Published online 1 FEB 2019

©2019. American Geophysical Union. All Rights Reserved.

This article has been contributed to by US Government employees and their work is in the public domain in the USA.

Millennial-Scale Vulnerability of the Antarctic Ice Sheet to Regional Ice Shelf Collapse

Daniel F. Martin¹ , Stephen L. Cornford^{2,3} , and Antony J. Payne³ 

¹Computational Research Division, Lawrence Berkeley National Laboratory, Berkeley, CA, USA, ²Department of Geography, College of Science, Swansea University, Swansea, UK, ³Centre for Polar Observation and Modelling, School of Geographical Sciences, University of Bristol, Bristol, UK

Abstract The Antarctic Ice Sheet (AIS) remains the largest uncertainty in projections of future sea level rise. A likely climate-driven vulnerability of the AIS is thinning of floating ice shelves resulting from surface-melt-driven hydrofracture or incursion of relatively warm water into subshef ocean cavities. The resulting melting, weakening, and potential ice shelf collapse reduces shelf buttressing effects. Upstream ice flow accelerates, causing thinning, grounding-line retreat, and potential ice sheet collapse. While high-resolution projections have been performed for localized Antarctic regions, full-continent simulations have typically been limited to low-resolution models. Here we quantify the vulnerability of the entire present-day AIS to regional ice shelf collapse on millennial timescales treating relevant ice flow dynamics at the necessary ~1-km resolution. Collapse of any of the ice shelves dynamically connected to the West Antarctic Ice Sheet (WAIS) is sufficient to trigger ice sheet collapse in marine-grounded portions of the WAIS. Vulnerability elsewhere appears limited to localized responses.

Plain Language Summary The biggest uncertainty in near-future sea level rise (SLR) comes from the Antarctic Ice Sheet. Antarctic ice flows in relatively fast-moving ice streams. At the ocean, ice flows into enormous floating ice shelves that push back on their feeder ice streams, buttressing them and slowing their flow. Melting and loss of ice shelves due to climate changes can result in faster-flowing, thinning, and retreating ice leading to accelerated rates of global SLR. To learn where Antarctica is vulnerable to ice shelf loss, we divided it into 14 sectors, applied extreme melting to each sector's floating ice shelves in turn, then ran our ice flow model 1,000 years into the future for each case. We found three levels of vulnerability. The greatest vulnerability came from attacking any of the three ice shelves connected to West Antarctica, where much of the ice sits on bedrock lying below sea level. Those dramatic responses contributed around 2 m of SLR. The second level came from four other sectors, each with a contribution between 0.5 and 1 m. The remaining sectors produced little to no contribution. We examined combinations of sectors, determining that sectors behave independently of each other for at least a century.

1. Introduction

The contribution of the Antarctic Ice Sheet (AIS) remains the largest source of uncertainty in projections of future sea level rise (SLR; Church et al., 2013). The flow of ice from the Antarctic interior to the sea is organized into networks of relatively fast-flowing (1–10 km/year) ice streams, which flow over submarine bedrock to feed large floating ice shelves (Figure 1). The boundary between *grounded* ice (ice thick enough to rest on submarine bedrock) and floating ice is known as the *grounding line* (GL), and it is this transitional region that must be treated with care in models of the AIS. (Cornford et al., 2016; Durand et al., 2009; Pattyn et al., 2013). Finally, ice enters the ocean either via basal melting (due to the presence of relatively warm and saline ocean water reaching the underside of floating ice), surface melting (via hydrofracture-driven crevasses), or through iceberg calving. In turn, ice shelves affect their feeder ice streams through a “buttressing” effect (Asay-Davis et al., 2016; Goldberg et al., 2009; Gudmundsson, 2013), slowing them and reducing their discharge. Ice shelf thinning and collapse lead to reduction or elimination of this buttressing effect, leading in turn to acceleration, thinning, and retreat of the ice sheet, particularly via the marine ice sheet instability (Schoof, 2007; Weertman, 1974). This has been both inferred from observations (Rignot et al., 2014) and demonstrated by modeling (Favier et al., 2014). Fürst et al. (2016) evaluated the buttressing effect in Antarctic ice shelves based on an analysis of their instantaneous stress state, which provides an indication

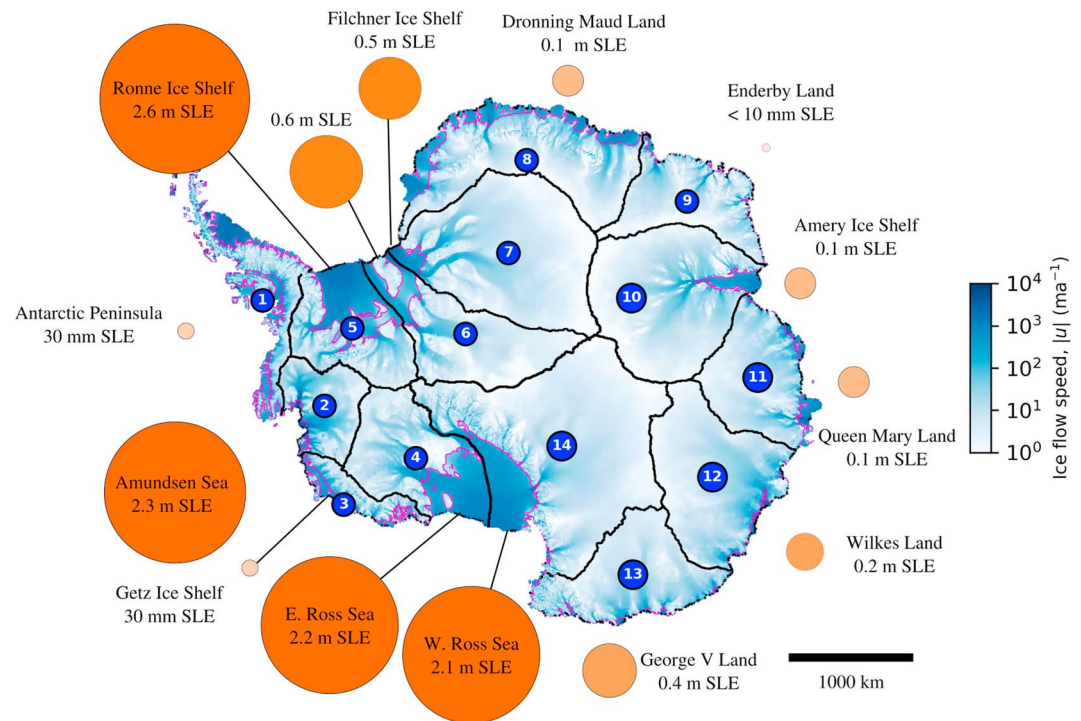


Figure 1. Antarctic vulnerability to localized ice shelf collapse. Initial modeled flow speed is shown in shaded blue. Magenta lines indicate initial grounding-line locations. Mass lost above flotation (eustatic sea level equivalent [SLE]) after 1,000 years of extreme, sustained ice shelf thinning originating in the numbered sectors is illustrated by the adjacent circle area.

of the short-term dynamic consequences of ice shelf collapse, but leaves open the question of the larger, longer-term effects once retreat has begun. How this retreat progresses will be dominated by effects like the marine ice sheet instability, which is dependent on the topography underlying the ice sheet. (Schoof, 2007; Weertman, 1974).

While high-resolution projections have been performed for localized Antarctic regions like the Pine Island and Thwaites glaciers (Favier et al., 2014; Waibel et al., 2018), simulations of the whole continent have typically been limited to low-resolution models. However, in recent years the accuracy of such projections from low-resolution models has been called into question. (Cornford et al., 2016; Durand et al., 2009; Pattyn et al., 2013; Reese et al., 2018). Here we use the BISICLES ice sheet model (Cornford et al., 2015), which deploys subkilometer mesh resolution in key zones, to simulate the response of the entire continental ice sheet to regional ice shelf collapse. Such fine resolution has been demonstrated to be necessary for the correct representation of the stresses at the GL, to the extent that numerical error can otherwise overshadow projections of AIS mass budget and stability (Cornford et al., 2013, 2016; Durand et al., 2009; Pattyn et al., 2013; Reese et al., 2018). BISICLES achieves this fine resolution through adaptive mesh refinement (AMR), dynamically deploying computationally expensive fine resolution only when and where needed to accurately resolve the evolving dynamics of the ice sheet.

Subjecting each and every ice shelf to extreme thinning, such that any floating ice is reduced to a thickness of 100 m within a few years of its detachment from the bed, leads to the complete collapse of the West Antarctic Ice Sheet (WAIS) and pronounced retreat in several East Antarctic basins, amounting to 4.6 m SLR over 500 years (Cornford et al., 2016). While this is an unrealistically high thinning rate, it does represent an upper bound on the rate of SLR due to continent-wide ice shelf thinning; by extension, it is natural to estimate the upper bound on the ice sheet's vulnerability to *regional* ice shelf collapse by, for example, confining such forcing to the Amundsen Sea Embayment, where ocean-induced retreat has already been observed (Rignot et al., 2014). We divided Antarctica into 14 sectors (Figure 1), corresponding to a broad-scale map of Antarctic ice drainage basins similar to that in Zwally et al. (2012). For each sector, we ran an experiment in which we applied extreme ice shelf thinning to any floating ice in the sector, evolving the ice sheet for 1,000 years.

Simulations with coupled ice sheet and ocean models (Asay-Davis et al., 2016) suggest that subshelf melt forcing will follow GLs as they retreat. Thus, melt forcing is allowed to follow GLs as they retreat into the interior of the continent, even out of the original sector. To test whether melt following the GL over such large-scale retreat was essential, we ran a second set of experiments in which this thinning was confined to the chosen sector. In some cases, GLs retreated out of the selected sector, at which point the forcing stopped and any further retreat was unforced. While our experiments implemented ice shelf weakening specifically due to submarine melting, surface melting like that seen on the Siple Coast in 2016 (Nicolas et al., 2017) can also result in weakening and eventual collapse of ice shelves, as observed in the Larsen B Ice Shelf breakup in 2002 (McGrath et al., 2012; van den Broeke, 2005). The effects of ice shelf loss in this work are independent of the specific form of shelf weakening; rather, they indicate the general vulnerability of the AIS to the weakening and loss of its floating ice shelves.

2. Methods

We began with the Antarctic “present-day” initial condition used in Cornford et al. (2016), which is based on the Bedmap2 data set (Fretwell et al., 2013). We use the present-day temperature field computed by Pattyn (2010) and the accumulation field from Arthern et al. (2006). Using the Antarctic sector map (1) as a mask, we applied the extreme melting scenario from Cornford et al. (2016) to any floating ice in the chosen sector(s) and then evolved the ice sheet in each melt configuration for 1,000 years using the BISICLES ice sheet model (Cornford et al., 2013). The AMR capabilities of the BISICLES model enabled us to apply sufficiently fine spatial and temporal resolution (as demonstrated in Cornford et al., 2016) to accurately resolve the GL dynamics of the ice sheet. The finest resolution (1 km) was applied near grounding lines, dynamically adapting the resolution and following the GLs as the solution evolved. This resolution, when coupled with a subgrid-friction scheme, has been demonstrated to be sufficient for this experiment in Cornford et al. (2016) and in the supporting information. The submarine melt forcing used in this work is depth dependent, ranging from no melting for ice shelves with a thickness less than 100 m, then linearly increasing with ice shelf draft up to a maximum ablation value of 400 m/year (m/a) where the ice thickness is greater than 800 m. (There is an error in the forcing function specified in Cornford et al. (2016)—The values here are the correct ones.) While this produces unrealistically high melt rates, the intent is to test the ice sheet’s sensitivity to forcing, not produce credible temporally accurate projections (which will be left to a following work). Limiting thinning to shelves with greater than 100-m thickness rather than thinning all the way to zero thickness is a numerical convenience. The supporting information includes a demonstration that the 100-m cutoff is thin enough to be dynamically similar to thinning all the way to zero, while avoiding a set of numerical difficulties that occasionally occur when portions of ice shelves are removed entirely. As recommended in Seroussi and Morlighem (2018), we confine melting to computational cells that are fully floating.

We performed two sets of experiments. In the first, the melt forcing associated with a given sector or sectors was allowed to follow the GL retreat anywhere within that sector or more than 100-km distant from the initial ice shelf region of another sector. In the second set, subshelf melt forcing was confined to the chosen sector or sectors. In a few cases (particularly sector 5), GLs passed out of the sector, at which point the melt forcing would no longer follow the GL retreat (but GLs were free to continue their retreat and did). We also ran a control experiment with no subshelf melting, which showed a tendency to gain ice after about 100 years, gaining 197 mm SLE after 500 years and 467 mm SLE after 1,000 years, primarily due to accumulation in the interior. While this control does not take present-day retreat and subshelf melting rates into account, the goal of this work is to evaluate vulnerability to *any* shelf weakening and collapse, including any which may already be underway, while the tendency of the control to add ice tends to isolate just the response due to the applied forcing, while not affecting the dynamics of the response. To isolate the effect of the melt-induced dynamics, we subtracted the control solution from the results of the runs. We then evaluated the change in the volume of ice over flotation, the net contribution to global sea levels.

While our experiment design aims to capture the important ice physics relevant to the dynamics of marine ice sheet instability, certain processes are not incorporated in our model. In this work, we do not incorporate the marine ice cliff instability proposed in Pollard et al. (2015) and DeConto and Pollard (2016), which remains controversial and has not been fully developed in a modeling context. Also, while we incorporate a realistic ice temperature field in our initial condition, we do not evolve that temperature field as the experiments progress. We believe this to be a reasonable approximation for much of this experiment given the

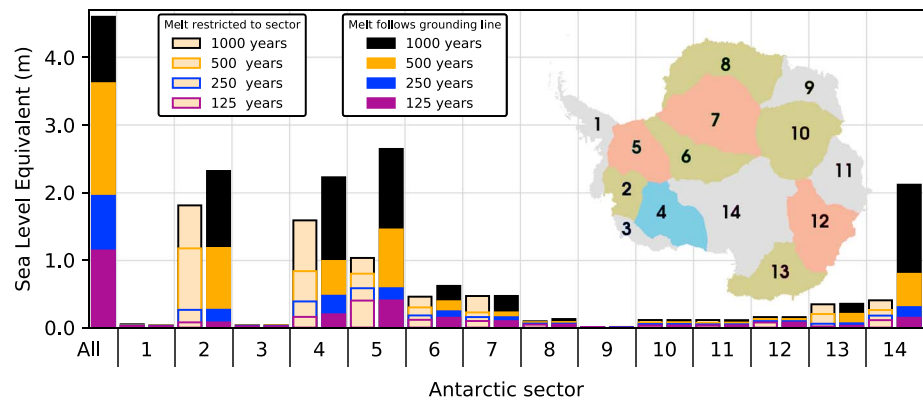


Figure 2. One-thousand-year contribution to sea level rise (in mm sea level equivalent) after 125,250, 500, and 1,000 years for each Antarctic sector. Results from both experiments are shown; for each sector, the left bar shows the case where melt is restricted to the specified sector, and the right bar shows the case where melt is allowed to follow grounding lines into other sectors. “All” is the case where there is melting in all sectors simultaneously.

rapid nature of the response compared to the relatively slow timescale of thermal evolution in the ice. At the same time, it is likely that this omission results in generally colder ice than would result from fully thermomechanically coupled simulations and so would tend to *underestimate* ice sheet response. Similarly, the basal friction field we compute to match our initial velocity field to observations remains fixed for the duration of the runs. While this is also not realistic, we expect it will primarily miss the tendency of bed friction to reduce as the GLs move inland, and ice flow becomes more active, which will also tend to underpredict acceleration, thinning, and retreat in the ice sheet.

Plots of ice thickness differences relative to the control and plots of contribution to SLR versus time for each case are provided in the supporting information.

3. Results

Figure 2 shows the contribution to SLR after 1,000 years due to shelf loss for each sector, compared to the control, which had no thinning, along with the result from forcing all sectors simultaneously, which resulted in a response of 4.6 m of eustatic sea level equivalent (SLE) after 1,000 years. In all cases, regional ice shelf collapse caused at least some enhanced Antarctic contribution to SLR when compared to the control. We observe three tiers of response. The first tier, comprising the largest responses, includes sectors 2 (the Amundsen Sea Embayment), 4 (the portion of the Ross Ice Shelf adjacent to Siple Coast streams), and 5 (the western part of the Ronne Ice Shelf) with or without out-of-sector melting, and sector 14 (the portion of the Ross ice shelf adjacent to the Transantarctic Mountains) if out-of-sector melting is permitted ranges from 2.2 to 2.6 m of SLE and comes from retreat chronologies in which GL retreat reaches the interior of the WAIS, as illustrated in Figure 3. The striking feature of these results is that all four high-impact cases trigger continental scale retreat in the same vulnerable submarine-grounded part of WAIS, but through different routes. As shown in Figure 3, forcing from sector 2 drains ice through the Thwaites Glacier basin into the Amundsen Sea, forcing from sector 5 drains ice through the Rutford Ice Stream into the Ronne Ice Shelf and ultimately the Weddell Sea, and forcing from sectors 4 and 14 drains into the Ross Sea. This result indicates the high degree of vulnerability of the marine-grounded portions of the WAIS to the weakening of any of its dynamically connected ice shelves and agree generally with Feldmann and Levermann (2015a), in which a similar study was conducted for a regional WAIS domain forced from the Amundsen Sea. Notably, sector 14 only has limited access to the vulnerable part of WAIS via the Whillans and Mercer ice streams, but depending on the evolution of shelf collapse as those GLs retreat, thinning in that sector can cause WAIS collapse similar to the more well-connected (to the WAIS interior) sectors. At the same time, its limited impact when melting remains in-sector underscores the difference between the level of vulnerability in the East Antarctic Ice Sheet (EAIS) and WAIS. This also highlights the nature of the Siple Coast as an effective route to WAIS collapse, which has yet to be extensively studied by current models. On the other hand, the limited-melt experiment results for sectors 2, 4, and 5 indicate a high degree of vulnerability of the WAIS

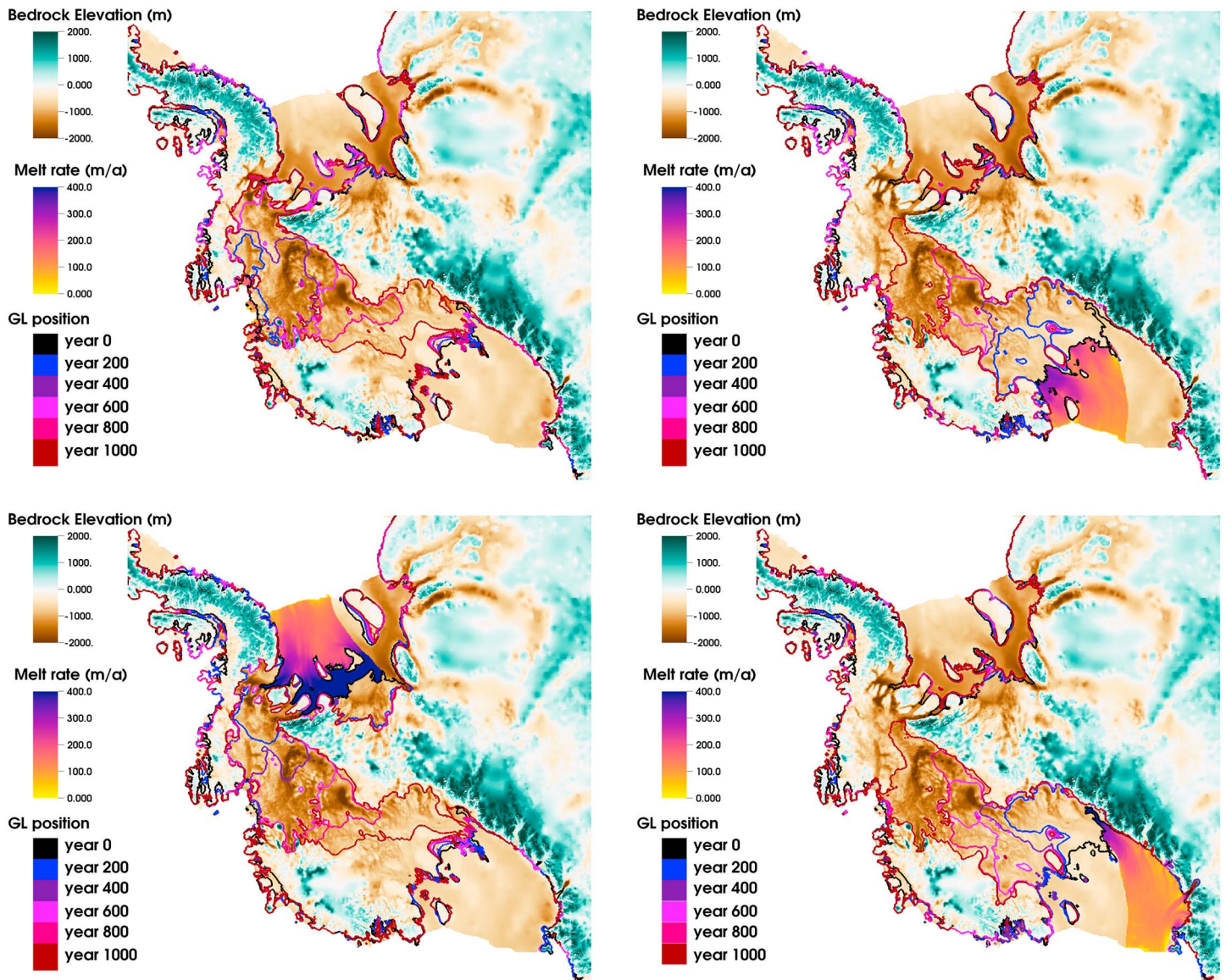


Figure 3. Grounding-line evolution illustrated with contours every 200 years for sectors 2 (upper left), 4 (upper right), 5 (lower left), and 14 (lower right). Colormap shows initial melt-forcing distribution for each case. GL = grounding line.

even to unforced retreat once retreating GLs breach the boundaries of the region, with much of the retreat and loss in the central WAIS occurring out of the originally forced sector.

The second tier of AIS response consists of ice streams whose cumulative contribution to SLR is comparable to the main WAIS system and is evident in Figure 2. Forcing applied to sectors 6 (including the Support Force and Foundation glaciers), 7 (the Bailey, Slessor, and Recovery ice streams flowing into the Filchner Ice Shelf), and 13 (George V land, including the Wilkes subglacial basin) results in 300–600 mm SLE in each case, as it does in sector 14 if melting does not progress beyond the sector (Figures S3, S4, and S7 in the supporting information). In all of these cases, only minimal effects are seen outside the immediately affected drainage basins.

The third tier comprises the remaining seven sectors, which each exhibit millennial ice losses of less than 200 mm SLE. A notable case is that of the Totten and Vanderford glaciers (in sector 12, Wilkes Land), which undergo rapid retreat at the start of the simulations but for which the relatively limited mass loss is ultimately restricted to the deep trough surrounding Law Dome. This suggests that the current activity observed in

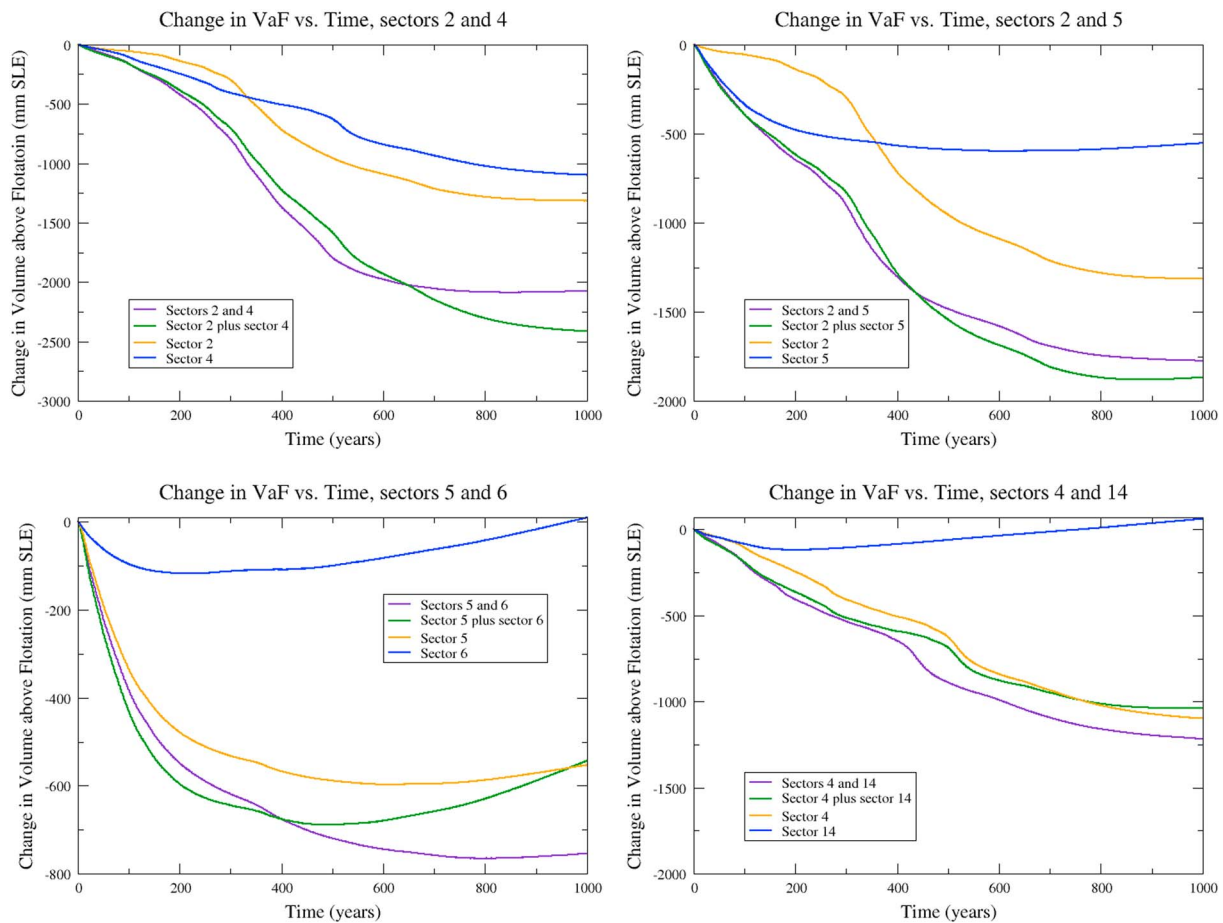


Figure 4. Change in volume above flotation (VaF; in mm sea level equivalent [SLE]) for selected combinations of sectors: (top left) sectors 2 and 4, (top right) sectors 2 and 5, (bottom left) sectors 5 and 6, and (bottom right) sectors 4 and 14. In each plot, the purple line is the case with both sectors forced simultaneously, green is the sum of the two independently forced values, and the orange and blue lines represent the individual sectors.

this sector (Rintoul et al., 2016; Xin et al., 2015) is not likely to result in large contributions to SLR in the long term.

Even with the extreme forcing employed in this experiment, most of the contribution to SLR occurs well after the first 100 years. The initial loss comprises small contributions from every sector of the ice sheet (all the way around the margin), whereas the the potential for larger, longer-term loss is dominated by the sectors that activate WAIS collapse.

3.1. Regional Independence

Due to limitations in computational resources, it is currently common practice to model individual AIS drainage basin evolution separately. For example, previous studies have examined the response of the Pine Island Glacier (Cornford et al., 2013; Favier et al., 2014), the Thwaites Glacier (Joughin et al., 2014; Seroussi et al., 2017; Waibel et al., 2018), or multiple glaciers in the same catchment (Cornford et al., 2015). On the other hand, studies that examine the entire AIS have tended to employ low spatial resolution and/or parameterized critical dynamical processes due to the prohibitive computational expense of modeling the entire ice sheet at high resolutions (DeConto & Pollard, 2016; Gollledge et al., 2015; Winkelmann et al., 2015). The validity of sea level projections based on regional simulations depends on the assumption of independence of the region in question from ice dynamics occurring elsewhere in the ice sheet, which may have questionable validity given the multiple vulnerabilities of the WAIS shown above. This type of interbasin interaction was examined in an idealized setting in Feldmann and Levermann (2015b). To test this in the Antarctic setting, we also subjected selected combinations of sectors to simultaneous melt forcing to determine whether different connected sectors of the WAIS truly evolve independently. We examine two configurations. In the first, we examine the regional independence of the first-tier sectors that directly drive WAIS collapse.

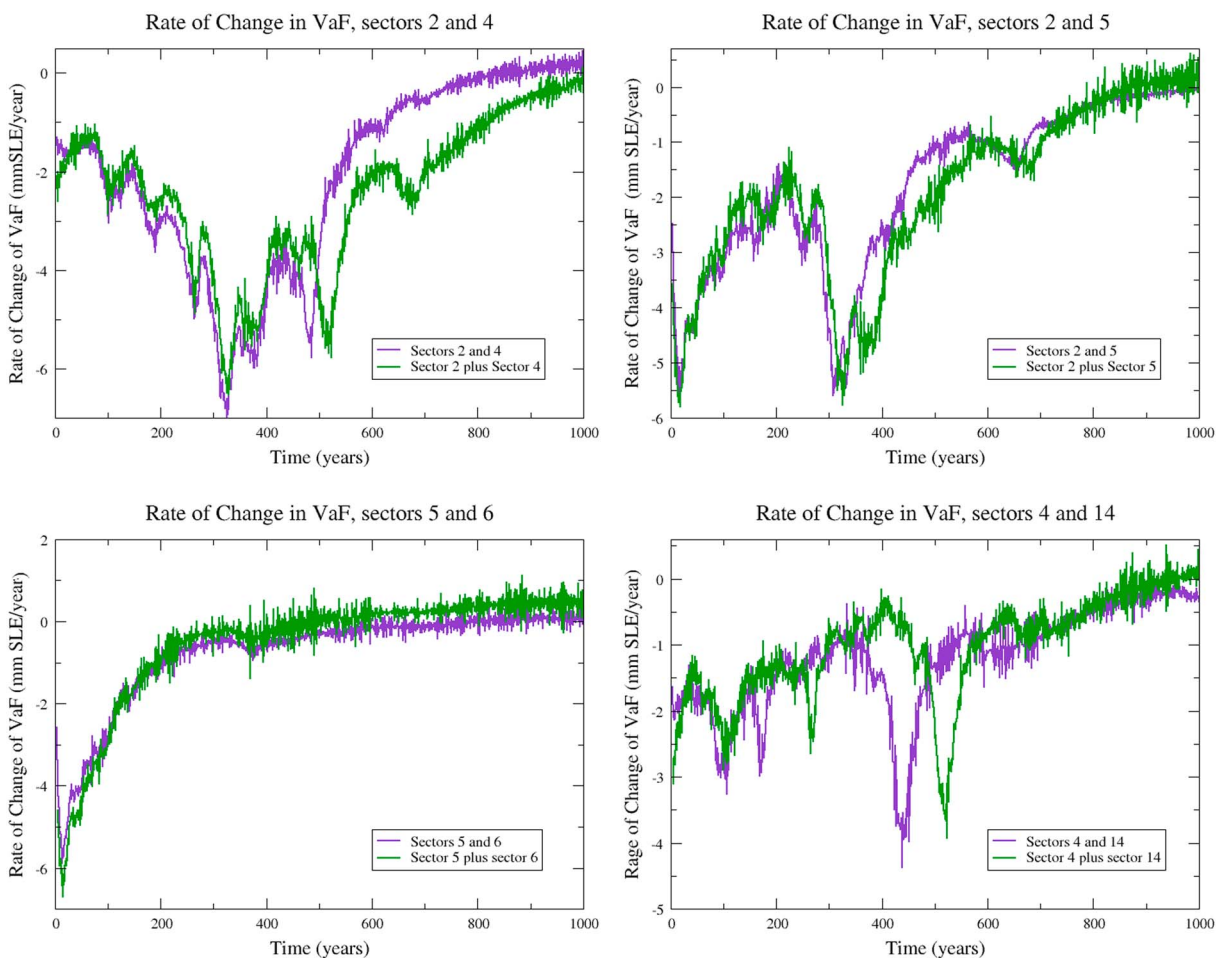


Figure 5. Rate of change in volume above flotation (VaF; in mm sea level equivalent [SLE]) for selected combinations of sectors: (top left) sectors 2 and 4, (top right) sectors 2 and 5, (bottom left) sectors 5 and 6, and (bottom right) sectors 4 and 14. Purple is both sectors simultaneously, and green is the sum of the two independently run values.

In particular, we examine the combinations of sectors 2 and 4 and 2 and 5. The third possible combination, 4 and 5, is less relevant due to the current active retreat in the ASE region (sector 2) but is included in the supplemental materials for completeness. The second configuration examines the independence of different parts of the large ice shelves (i.e., the combinations of sectors 5 and 6 and sectors 4 and 14). Time-dependent plots of the volume above flotation (i.e., the contribution to SLR) are shown in Figure 4 while the rate of change of volume above flotation (rate of contribution to SLR) is shown in Figure 5. If ice dynamics for each sector are independent, then the results of the combined run (purple lines in Figures 4 and 5) and the sum of the individual runs (green lines in Figures 4 and 5) should be identical. As seen in Figure 4, this generally holds true in WAIS-connected sectors for about 100 years, after which the assumption of regional independence appears to break down somewhat as small differences appear. The differences remain small for a further 300–400 years time, at which point GLs retreat significantly out of their original drainage basins and the independent runs begin to contend for the same grounded ice, and so can no longer be treated additively.

The exception to this is for the Ronne Ice shelf sectors, (Figure 4, lower left) where WAIS collapse is entirely due to forcing in the western part of sector 5 but the most dramatic, near-future retreat, associated with the Möller and Institute ice streams, is hastened by the inclusion of forcing in the eastern part of sector 6.

In general, distinguishable “events” in the plots in Figure 5—such as WAIS collapse when rates of SLR grow to 5 mm/a—occur earlier when both sectors are forced, suggesting that temporally detailed projections of sea level contributions for timescales longer than centennial may require the use of whole-continent (or at least whole-WAIS/EAIS) models. It is, however, also possible that realistic forcing scenarios will preserve

dynamic independence (and thus the validity of regional modeling) longer, given the extreme nature of the applied forcing in this set of experiments.

4. Discussion and Conclusions

In summary, we find that the primary Antarctic vulnerability to submarine melting, and shelf collapse remains the collapse of the WAIS. There are three primary routes to WAIS collapse. Beyond the currently active vulnerability to retreat in the Amundsen Sea Sector, we also find that the WAIS is vulnerable to weakening or collapse of the Ronne Ice Shelf via the Rutford Ice Stream, as well as a broader vulnerability via the ice streams of the Siple Coast. The remaining vulnerabilities, particularly in the EAIS, are much smaller and are regionally contained. This tends to confirm earlier studies performed with coarse-grid, heavily parameterized models. While this work clarifies the vulnerability of the AIS, placing what is likely an upper bound on its response to local incursions of circumpolar deep water or surface-melt-driven hydrofracture, it falls to global circulation models and ocean models (especially those with active ice-ocean coupling) to quantify the likelihood and timing of such shelf-collapse forcing (such as the warm-water incursion predicted by Hellmer et al., 2017, for the Weddell Sea ice shelves), and the potential coupling with shelf weakening due to surface-melt driven hydrofracture. We also find that at least for the cases examined in this work, regional ice sheet models are likely sufficient for these projections for 400–500 years for broadly characterizing ice sheet response, but whole ice sheet models may be required for time-accurate projections beyond the century scale.

Code and Data Availability

We used the publicly available version of the BISICLES ice sheet model code, release version 1.0. Instructions for downloading and installing BISICLES may be found in the “getting started” section at <http://bisicles.lbl.gov>. BISICLES is written in a combination of C++ and FORTRAN and is built upon the Chombo AMR software framework. More information about Chombo may be found at <http://Chombo.lbl.gov>.

Data, input, and configuration files for the runs in this work are available at <http://portal.nersec.gov/project/iceocean/AntarcticRegionalMelt/>

Acknowledgments

The authors gratefully acknowledge input from Stephen Price, Matthew Hoffman, and Esmond Ng. We also thank the two anonymous reviewers, whose thoughtful suggestions improved this work. Work at LBL was supported by the Director, Office of Science, Offices of Advanced Scientific Computing Research (ASCR) and Biological and Environmental Research (BER), of the U.S. Department of Energy under contract No. DE-AC02-05CH11231, as a part of the ProSpect SciDAC Partnership. This research used resources of the National Energy Research Scientific Computing Center, a DOE Office of Science User Facility supported by the Office of Science of the U.S. Department of Energy under contract No. DE-AC02-05CH11231.

References

- Arthern, R. J., Winebrenner, D. P., & Vaughan, D. G. (2006). Antarctic snow accumulation mapped using polarization of 4.3-cm wavelength microwave emission. *Journal of Geophysical Research*, *111*, D06107. <https://doi.org/10.1029/2004JD005667>
- Asay-Davis, X. S., Cornford, S. L., Durand, G., Galton-Fenzi, B. K., Gladstone, R. M., Gudmundsson, G. H., et al. (2016). Experimental design for three interrelated marine ice sheet and ocean model intercomparison projects: MISMIP v. 3 (MISMIP+), ISOMIP v. 2 (ISOMIP+) and MISOMIP v. 1 (MISOMIP1). *Geosci. Model Dev.*, *9*(7), 2471–2497. <https://doi.org/10.5194/gmd-9-2471-2016>
- Church, J. A., Clark, P. U., Cazenave, A., Gregory, J. M., Jevrejeva, S., Levermann, A., et al. (2013). Sea level change, *Climate change 2013: The physical science basis. contribution of working group i to the fifth assessment report of the intergovernmental panel on climate change* (pp. 1137–1216). Cambridge, United Kingdom and New York, NY: Cambridge University Press. <https://doi.org/10.1017/CBO9781107415324.026>
- Cornford, S. L., Martin, D. F., Graves, D. T., Ranken, D. F., Le Brocq, A. M., Gladstone, R. M., et al. (2013). Adaptive mesh, finite volume modeling of marine ice sheets. *Journal of Computational Physics*, *232*(1), 529–549.
- Cornford, S. L., Martin, D. F., Lee, V., Payne, A. J., & Ng, E. G. (2016). Adaptive mesh refinement versus subgrid friction interpolation in simulations of Antarctic ice dynamics. *Annals of Glaciology*, *57*(73), 1–9. <https://doi.org/10.1017/aog.2016.13>
- Cornford, S. L., Martin, D. F., Payne, A. J., Ng, E. G., Le Brocq, A. M., Gladstone, R. M., et al. (2015). Century-scale simulations of the response of the West Antarctic Ice Sheet to a warming climate. *The Cryosphere*, *9*(4), 1579–1600.
- DeConto, R. M., & Pollard, D. (2016). Contribution of Antarctica to past and future sea-level rise. *Nature*, *531*, 591–597. <https://doi.org/10.1038/nature17145>
- Durand, G., Gagliardini, O., Zwinger, T., Meur, E. L., & Hindmarsh, R. C. (2009). Full Stokes modeling of marine ice sheets: Influence of the grid size. *Annals of Glaciology*, *50*(52), 109–114. <https://doi.org/10.3189/172756409789624283>
- Favier, L., Durand, G., Cornford, S. L., Gudmundsson, G. H., Gagliardini, O., Gillet-Chaulet, F., et al. (2014). Retreat of Pine Island Glacier controlled by marine ice-sheet instability. *Nature Climate Change*, *5*(2), 1–5. <https://doi.org/10.1038/nclimate2094>
- Feldmann, J., & Levermann, A. (2015a). Collapse of the West Antarctic Ice sheet after local destabilization of the Amundsen Basin. *Proceedings of the National Academy of Sciences*, *112*(46), 14,191–14,196.
- Feldmann, J., & Levermann, A. (2015b). Interaction of marine ice-sheet instabilities in two drainage basins: Simple scaling of geometry and transition time. *The Cryosphere*, *9*(2), 631–645. <https://doi.org/10.5194/tc-9-631-2015>
- Fretwell, P., Pritchard, H. D., & Vaughan, D. G. (2013). Bedmap2: improved ice bed, surface and thickness datasets for Antarctica. *The Cryosphere*, *7*(1), 375–393. <https://doi.org/10.5194/tc-7-375-2013>
- Fürst, J. J., Durand, G., Gillet-Chaulet, F., Tavard, L., Rankl, M., Braun, M., & Gagliardini, O. (2016). The safety band of Antarctic ice shelves. *Nature Climate Change*, *6*(5), 479–482.

- Goldberg, D., Holland, D. M., & Schoof, C. (2009). Grounding line movement and ice shelf buttressing in marine ice sheets. *Journal of Geophysical Research*, *114*, F04026. <https://doi.org/10.1029/2008JF001227>
- Golledge, N. R., Kowalewski, D. E., Naish, T. R., Levy, R. H., Fogwill, C. J., & Gasson, E. G. W. (2015). The multi-millennial Antarctic commitment to future sea-level rise. *Nature*, *526*(7573), 421–425.
- Gudmundsson, G. H. (2013). Ice-shelf buttressing and the stability of marine ice sheets. *The Cryosphere*, *7*(2), 647–655. <https://doi.org/10.5194/tc-7-647-2013>
- Hellmer, H. H., Kauker, F., Timmermann, R., & Hattermann, T. (2017). The fate of the Southern Weddell Sea continental shelf in a warming climate. *Journal of Climate*, *30*, 4337–4350. <https://doi.org/10.1175/JCLI-D-16-0420.1>
- Joughin, I., Smith, B. E., & Medley, B. (2014). Marine ice sheet collapse potentially under way for the Thwaites Glacier Basin, West Antarctica. *Science*, *344*(6185), 735–738.
- McGrath, D., Steffen, K., Rajaram, H., Scambos, T., Abdalati, W., & Rignot, E. (2012). Basal crevasses on the Larsen C Ice Shelf, Antarctica: Implications for meltwater ponding and hydrofracture. *Geophysical Research Letters*, *39*, L16504. <https://doi.org/10.1029/2012GL052413>
- Nicolas, J. P., Vogelmann, A. M., Scott, R. C., Wilson, A. B., Cadeddu, M. P., Bromwich, D. H., et al. (2017). January 2016 extensive summer melt in West Antarctica favoured by strong El Niño. *Nature Communications*, *8*, 15799. <https://doi.org/10.1038/ncomms15799>
- Pattyn, F. (2010). Antarctic subglacial conditions inferred from a hybrid ice sheet/ice stream model. *Earth and Planetary Science Letters*, *295*(3), 451–461. <https://doi.org/10.1016/j.epsl.2010.04.025>
- Pattyn, F., Perichon, L., Durand, G., Favier, L., Gagliardini, O., Hindmarsh, R. C., et al. (2013). Grounding-line migration in plan-view marine ice-sheet models: Results of the ice2sea MISMIP3d intercomparison. *Journal of Glaciology*, *59*(215), 410–422. <https://doi.org/10.3189/2013JG12J129>
- Pollard, D., DeConto, R. M., & Alley, R. B. (2015). Potential Antarctic Ice Sheet retreat driven by hydrofracturing and ice cliff failure. *Earth and Planetary Science Letters*, *412*, 112–121. <https://doi.org/10.1016/j.epsl.2014.12.035>
- Reese, R., Winkelmann, R., & Gudmundsson, G. H. (2018). Grounding-line flux formula applied as a flux condition in numerical simulations fails for buttressed Antarctic ice streams. *The Cryosphere Discussions*, *2018*, 1–22. <https://doi.org/10.5194/tc-2017-289>
- Rignot, E., Mouginot, J., Morlighem, M., Seroussi, H., & Scheuchl, B. (2014). Widespread, rapid grounding line retreat of Pine Island, Thwaites, Smith, and Kohler glaciers, West Antarctica, from 1992 to 2011. *Geophysical Research Letters*, *41*, 3502–3509. <https://doi.org/10.1002/2014GL060140>
- Rintoul, S. R., Silvano, A., Pena-Molino, B., van Wijk, E., Rosenberg, M., Greenbaum, J. S., & Blankenship, D. D. (2016). Ocean heat drives rapid basal melt of the Totten Ice Shelf. *Science Advances*, *2*(12). <https://doi.org/10.1126/sciadv.1601610>
- Schoof, C. (2007). Ice sheet grounding line dynamics: Steady states, stability, and hysteresis. *Journal of Geophysical Research*, *112*, F03S28. <https://doi.org/10.1029/2006JF000664>
- Seroussi, H., & Morlighem, M. (2018). Representation of basal melting at the grounding line in ice flow models. *The Cryosphere*, *12*(10), 3085–3096. <https://doi.org/10.5194/tc-12-3085-2018>
- Seroussi, H., Nakayama, Y., Larour, E., Menemenlis, D., Morlighem, M., Rignot, E., & Khazendar, A. (2017). Continued retreat of Thwaites Glacier, West Antarctica, controlled by bed topography and ocean circulation. *Geophysical Research Letters*, *44*, 6191–6199. <https://doi.org/10.1002/2017GL072910>
- van den Broeke, M. (2005). Strong surface melting preceded collapse of Antarctic Peninsula ice shelf. *Geophysical Research Letters*, *32*, L12815. <https://doi.org/10.1029/2005GL023247>
- Waibel, M. S., Hulbe, C. L., Jackson, C. S., & Martin, D. F. (2018). Rate of mass loss across the instability threshold for Thwaites Glacier determines rate of mass loss for entire basin. *Geophysical Research Letters*, *45*, 809–816. <https://doi.org/10.1002/2017GL076470>
- Weertman, J. (1974). Stability of the junction of an ice sheet and an ice shelf. *Journal of Glaciology*, *13*, 3–13.
- Winkelmann, R., Levermann, A., Ridgwell, A., & Caldeira, K. (2015). Combustion of available fossil fuel resources sufficient to eliminate the Antarctic Ice Sheet. *Science Advances*, *1*(8), e1500589–e1500589.
- Xin, L., Eric, R., Mathieu, M., Jeremie, M., & Bernd, S. (2015). Grounding line retreat of Totten Glacier, East Antarctica, 1996 to 2013. *Geophysical Research Letters*, *42*, 8049–8056. <https://doi.org/10.1002/2015GL065701>
- Zwally, H. J., Giovinetto, M. B., Beckley, M. A., & Saba, J. J. L. (2012). Antarctic and Greenland drainage systems (*Tech. rep.*): GSFC Cryospheric Sciences Laboratory.